Proc. Indian Acad. Sci., Vol 87 A (E & P Sciences), No. 3, March 1978, pp. 29–45,

Incursion of the Pacific Ocean Water into the Indian Ocean

G S SHARMA*, A D GOUVEIA and SHUBHA SATYENDRANATH
National Institute of Oceanography, Dona Paula 403 004, Goa
*Present Address: Department of Marine Sciences, University of Cochin, Foreshore Road, Cochin 682 016

MS received 25 July 1977; in final form 17 November 1977

Abstract. Using the data collected during the International Indian Ocean Expedition, maps showing the distribution of depth, acceleration potential, salinity and oxyty were prepared for the northeast monsoon for the four potential thermosteric anomaly surfaces: 160, 120, 80 and 60 cl/t. Zonal components of current along 84°E were computed from the geopotential dynamic heights. From such an analysis, it became clear that low-salinity water from the Pacific intrudes into the western Indian Ocean through the Banda and Timor seas in the upper layers above 100 cl/t surface, while the North Indian Ocean Water penetrates towards the Eastern Archipelago below 100 cl/t surface. The South Equatorial Countercurrent and the Tropical Countercurrent are well depicted on the vertical section of zonal components as well as on the distribution of acceleration potential.

Keywords. Ocean expedition; depth distribution; acceleration potential; oxyty.

1. Introduction

As early as 1942 Sverdrup *et al* (1942) remarked that at the Dana Station 3849, located to the southwest of Sumatra, the low-salinity water of temperature higher than 10°C is probably of Pacific origin. Wyrtki (1957), for the first time, identified the Pacific Ocean Water in the Indian Ocean. Subsequently, its presence was confirmed by Wyrtki (1961), Taft (1963) and Sharma (1972). Warren *et al* (1966) considered that the low-salinity water at intermediate depths in the northwestern Indian Ocean could be the Subtropical Subsurface Water, and concluded that the Pacific Ocean would not be the source of the low-salinity water in the western Indian Ocean. Tchernia *et al* (1958) suggested this water to be the Antarctic Intermediate Water. In view of these differences of opinion, we have made a critical examination of incursion of the Pacific Ocean Water into the Indian Ocean by studying the geostrophic flow and the distribution of water properties on potential thermosteric anomaly surfaces at intermediate depths.

The South Equatorial Countercurrent discovered by Reid (1959) and the Tropical countercurrent (called Subtropical Countercurrent by Yoshida and Kidokoro 1967a, 1967b; Uda and Hasunuma 1969) could be traced on meridional sections by Sharma (1976a). But their presence either on level surfaces or steric surfaces could not be clearly demonstrated in the Indian Ocean, probably because of either paucity of data (Taft 1963; Sharma 1972) or averaging over vast areas just as in the International Indian Ocean Expedition Atlas (Wyrtki 1971). Hence an examination of the presence of these two currents in the geostrophic flow at different potential thermosteric anomaly surfaces has been considered essential.

2. Treatment of the material

This study is based on the data collected during the International Indian Ocean Expedition at 90 stations from various ships. Table 1 lists all the stations, and their geographical positions are shown in figure 1. All the stations were occupied during the northeast monsoon. The choice of the stations was made on the basis of their geographical distribution and the depth of observation. Preference was given for meridional sections from single cruises and stations which were worked in a single year. Because of abnormality in the weather as well as in oceanographical conditions in 1963 (Uda and Nakamura 1973), the data collected in 1963 were avoided as far as possible.

Potential temperature for each sample of all stations was computed using nomograms prepared by R B Montgomery and M J Pollak from Helland-Hansen's computations (1930). For each station, potential temperature was plotted against depth, salinity and oxyty on a grid with overprinted isopleths of thermosteric anomaly. The values of depth, salinity and oxyty at each chosen potential thermosteric anomaly surface were read directly from the station curves.

Geostrophic flow along the surfaces was deduced from the gradient of acceleration potential (Montgomery 1937; Montgomery and Spilhaus 1941; Montgomery and Stroup 1962) or Montgomery function as it has often been termed (Reid 1965). The expression of acceleration potential used for numerical computation is

$$\int_{\delta_{\theta_0}}^{\delta_\theta} P\, d\,\delta_\theta + P_0\,\delta_{\theta_0}$$

where δ_{θ_0} is potential thermosteric anomaly at the reference pressure (p_0). The reference pressure for this numerical integration has been chosen to be 2,000 db.

The distribution of properties and the geostrophic flow along surfaces of 160, 120, 80 and 60 cl/t are presented in figures 2 to 9. In order to have a quantitative estimate of the flow and also the depth to which a particular flow is consistent, zonal components of current at 84°E were estimated from geopotential dynamic heights and these have been presented in figure 10. The presentation of the geostrophic flow through the vertical section is adapted from Montgomery and Stroup (1962). The width of

Table 1. List of stations and cruise abbreviations used in figure 1, from International Indian Ocean Expedition.

Vessel and expedition	No. of stations used	Period	Abbreviation
Argo Lusiad III	1	Dec. 11, 1962	Ar
Atlantis Cruise 8	2	Nov. 6-8, 1963	An
Diamantina Cruise 4/62	7	Oct. 24-Nov. 10, 1962	Dm
Discovery IIOE Cruise 3	7	Mar. 20-Apr. 10, 1964	Di
Kagoshima Maru	12	Dec. 7, 1963-Jan. 9, 1964	Kg
Koyo Maru Cruise 14	7	Nov. 30, 1962-Jan. 1, 1963	Ko
Koyo Maru Cruise 16	4	Jan. 20-25, 1964	Ko
Umitaka Maru	9	Jan. 5-22, 1964	Ut
Vityaz Cruise 31	19	Dec. 19, 1959-Mar. 22, 1960	Vi
Vityaz Cruise 33	22	Dec. 11, 1960-Jan 10, 1961	Vi

Stations circled in figure 1 relate to computation of zonal components of the currents.

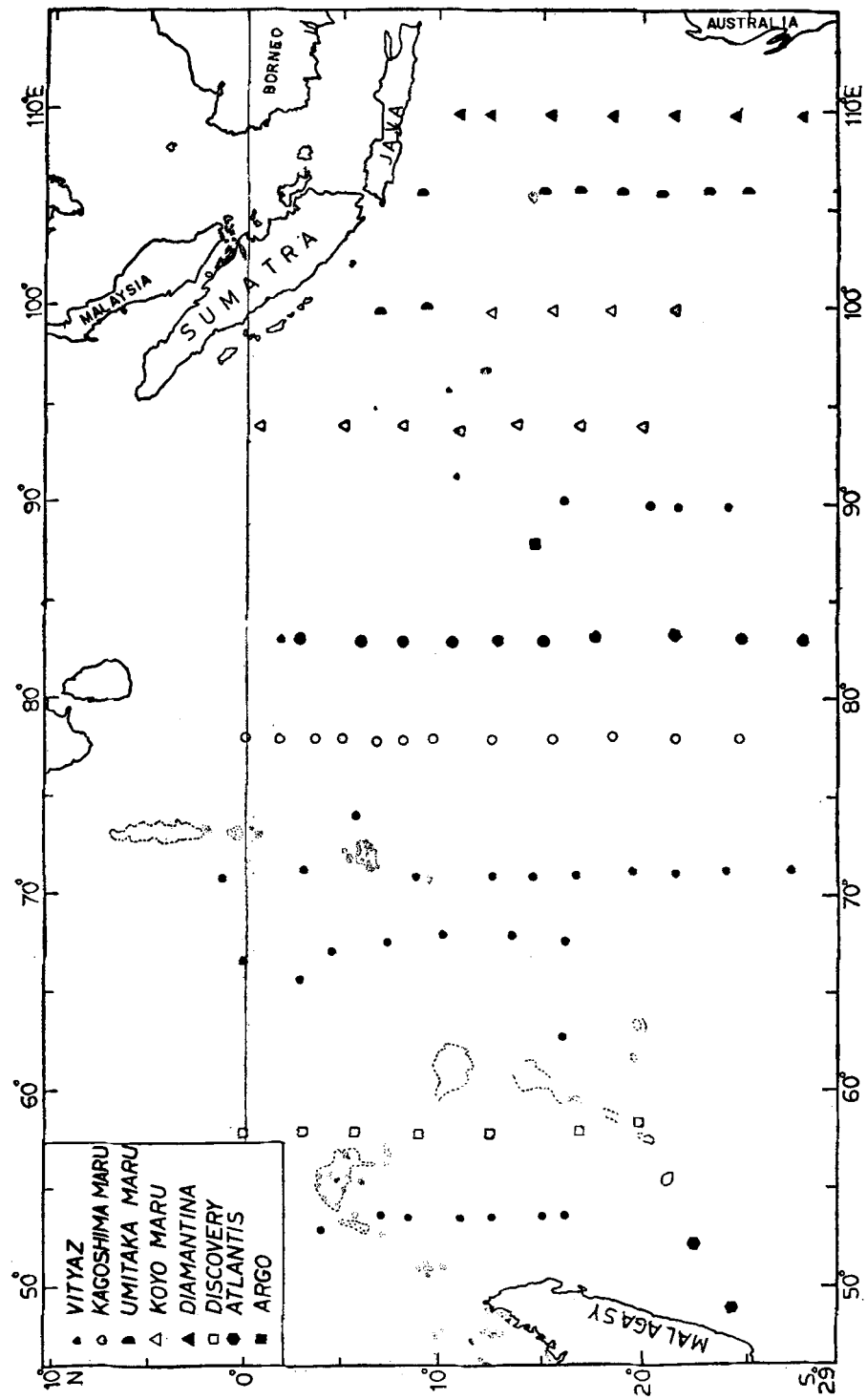

Figure 1. Station positions (See table 1).

the band represents the magnitude, and the sign is represented by shaded and stippled bands.

3. Distribution of properties on potential isanosteric surfaces

3.1. *Depth*

Northward from 20°S, 160 cl/t surface slopes upward a ridge associated with the northern boundary of the South Equatorial Current. The ridge is shallowest between 60°E and 75°E. In general, this surface slopes up slightly westward (figure 2a). The trough noticed on 160 cl/t surface along 20°S is not traced on 120 cl/t, perhaps

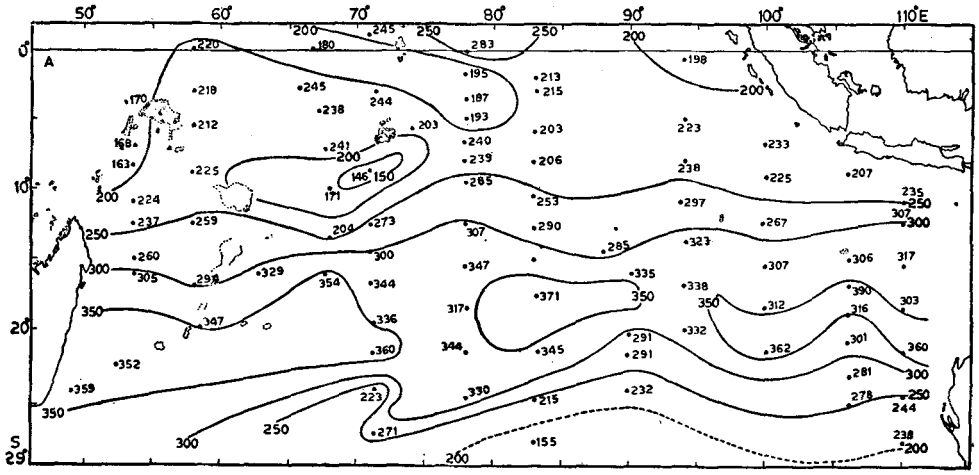

(a)

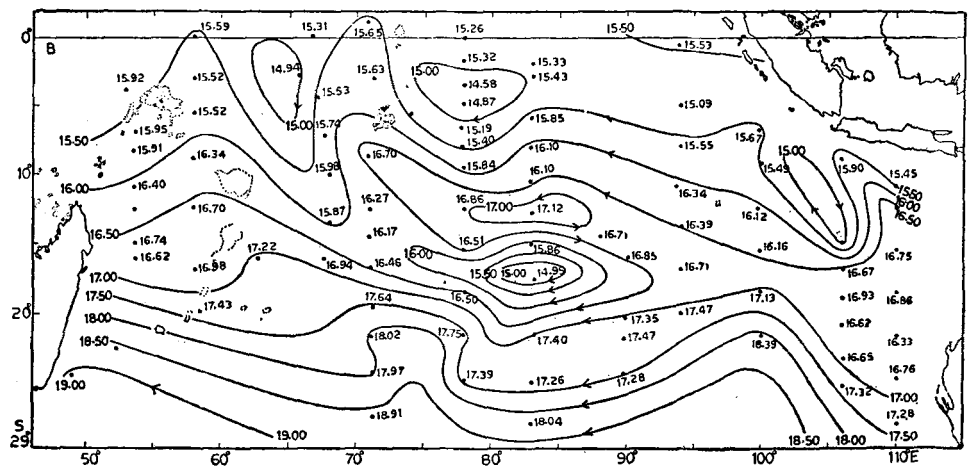

(b)

Figure 2. Depth in metres (a) acceleration potential (joules/kg) relative to 2,000 db (b) at $\delta_\theta = 160$ cl/t.

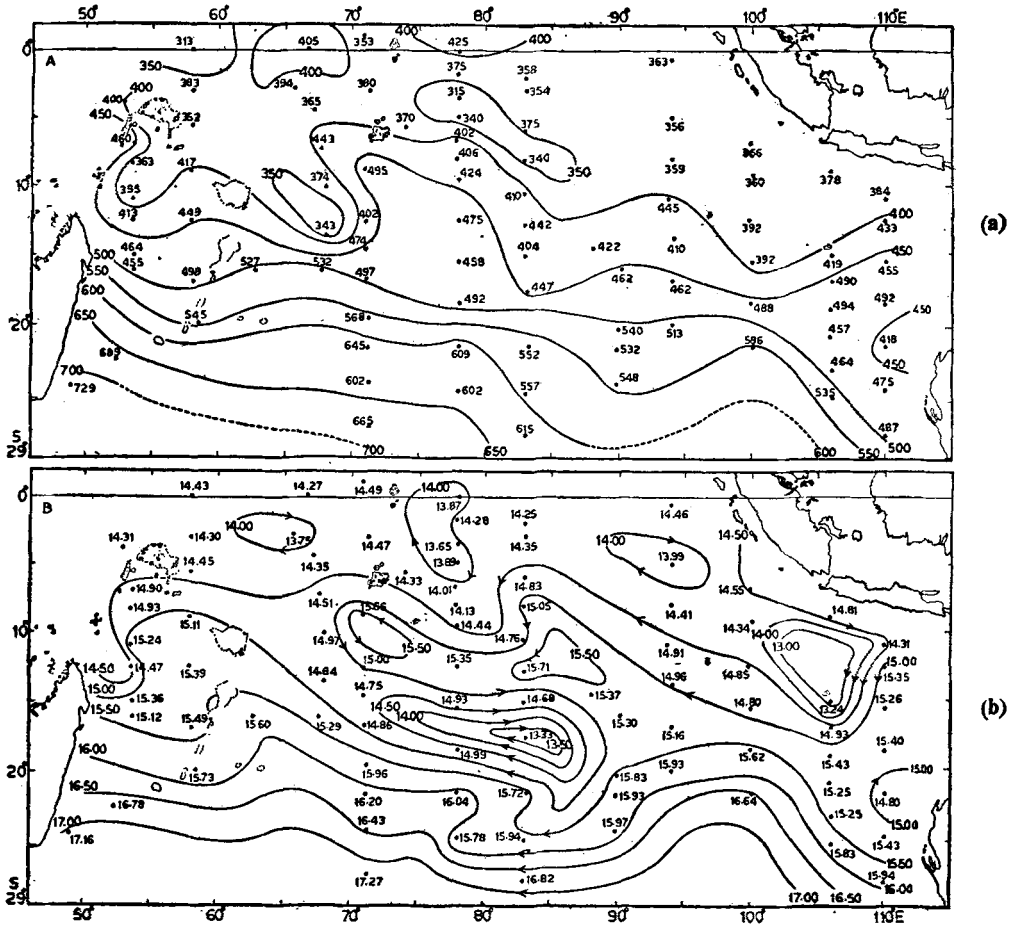

Figure 3. Depth in metres (a) acceleration potential (joules/kg) relative to 2,000 db (b) at $\delta\theta = 120$ cl/t.

because of its southward shift. A trough with depths ranging from 500 to 700 m, is located between 20°S and 35°S on 125 cl/t potential isosteric surface (Taft 1963, figure 4). The ridge, present slightly north of 10°S on 160 cl/t surface, is also noticed on 120 cl/t surface, slightly northward but in a distorted manner.

The lower surfaces (80 and 60 cl/t) slope meridionally more steeply than the upper surfaces (160 and 120 cl/t). The distribution pattern of depth on the surfaces of 80 and 60 cl/t varies markedly from that of 160 and 120 cl/t surfaces. On the former surfaces, between 10°S and 20°S, there are alternate troughs and ridges of small scale. Conspicuously, the orientation of depth contours of the surfaces 80 and 60 cl/t are similar. In the easternmost area of the study, the steep ridges on these surfaces, probably indicate the reversal of the flow in this region from that of the upper steric surfaces. The ridges along 15°S and the troughs at about 10°S, approximately, mark the southern and northern boundaries of the South Equatorial Countercurrent.

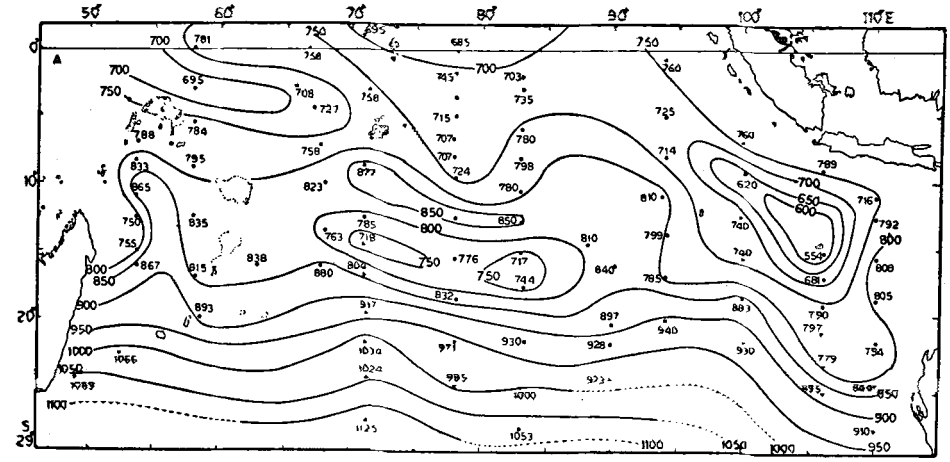

(a)

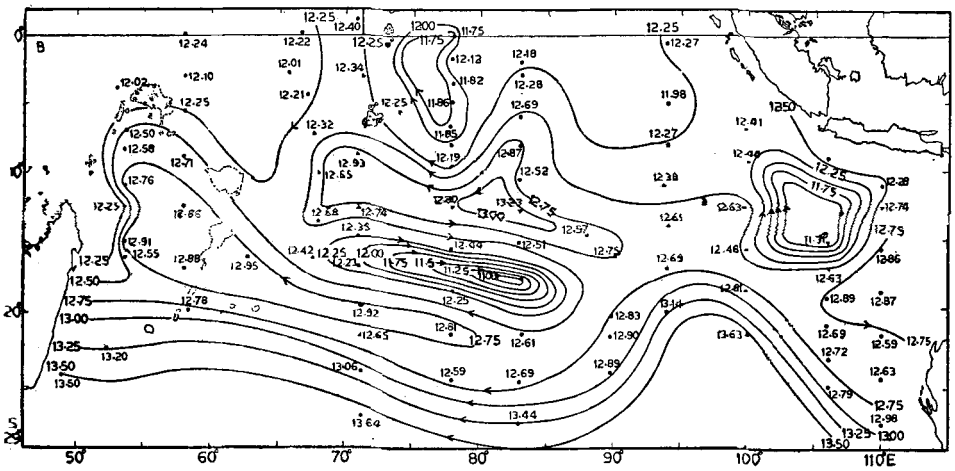

(b)

Figure 4. Depth in metres (a) acceleration potential (joules/kg) relative to 2,000 db (b) at $\delta_\theta = 80$ cl/t.

3.2. *Acceleration potential*

The distribution of acceleration potential (figures 2b, 3b, 4b, 5b) relative to 2,000 db clearly reveals the South Equatorial Countercurrent between 12°S and 15°S in the central region on all surfaces. There is a slight southward shift of the core of this current with lower steric levels. The northern and southern boundaries of this current are indicated by the maximum and minimum values of acceleration potential. The eastward flowing Tropical Countercurrent, located between 22°S and 26°S (Sharma 1976a), is evident on 80 and 60 cl/t surfaces by the lower values of acceleration potential south of 20°S. The isopleths of acceleration potential, if drawn at a closer interval would have certainly given a clearer evidence of the Tropical Countercurrent. Its presence is more prominent and spreads over the whole width of the ocean at lower steric levels. Nevertheless, relatively lower values of acceleration potential between

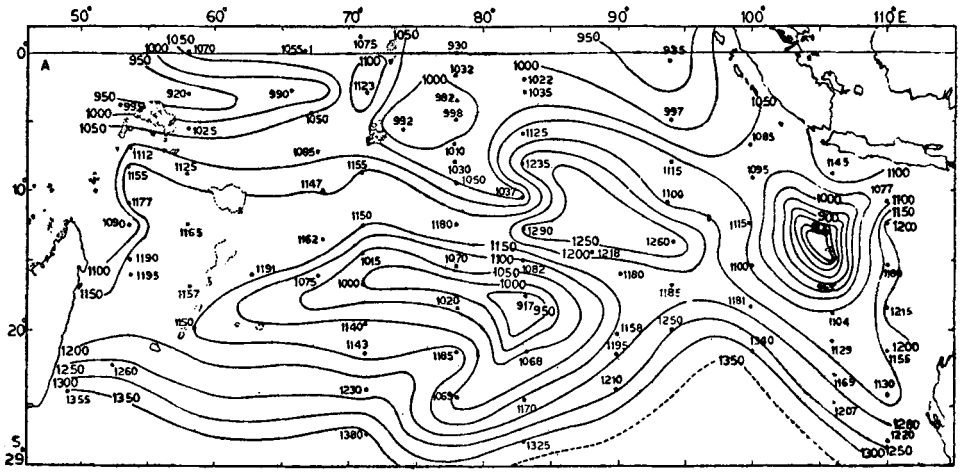

(a)

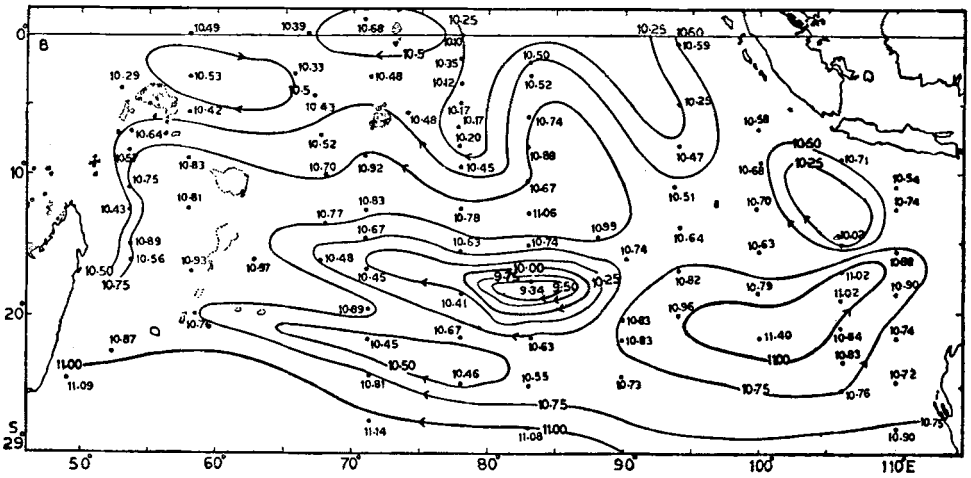

(b)

Figure 5. Depth in metres (a) acceleration potential (joules/kg) relative to 2,000 db (b) at $\delta\theta = 60$ cl/t.

21°S and 25°S on 160 and 120 cl/t surfaces are consistent with the presence of the Tropical Countercurrent located at these latitudes.

On 160 cl/t surface, there is an inconsistency between the distribution of acceleration potential and depth in the southernmost area under study. While this surface slopes up southward, the acceleration potential is seen to be increasing (figure 2b) in contrast to the general increase of acceleration potential at any surface with the increase of its depth. The reason for such a deviation on this surface alone is not immediately known. Probably, this surface may be in the layer of transition between two layers of opposing flows. The geopotential topography charts at 100 db and 300 db surfaces relative to 1,000 db during November and December reveal the opposing flows between 20°S and 25°S (Wyrtki 1971, pp. 375-381).

The geostrophic flow on 160 and 120 cl/t surfaces is mostly zonal, whereas in the

central equatorial region there is an indication of transequatorial flow on 80 and 60 cl/t surfaces. Just as the distribution of depth the acceleration potential distribution in the easternmost region under study reveals a marked variation in the flow pattern between the upper (160 cl/t, 120 cl/t) and the lower (80 cl/t, 60 cl/t) surfaces (figures 2b, 3b, 4b, 5b). Down the stream, west of 70°E, the South Equatorial Current branches northward to join the Equatorial Countercurrent, and southward to flow along the coast of Malagasy (figures 3b, 4b, 5b).

3.3. *Salinity*

The most striking feature in the distribution of salinity is, consistent with the distribution of depth and acceleration potential, similarity between 160 and 120 cl/t surfaces, and between 80 and 60 cl/t surfaces.

In the South Indian Ocean, the dominant water type in the thermocline is the Tropical Water which is formed in the surface salinity maximum (above 160 cl/t). Below this surface, its predominance is decreased with depth. At 120 cl/t the salinity maximum of the tropical origin, noticed on 160 cl/t is weakened and also shifted northward. There is no salinity maximum either at 80 or 60 cl/t at these latitudes (15°S–25°S).

The low-salinity tongues, extending along 11°S from 110°E as far west as 53°E and 70°E on 160 cl/t and 120 cl/t surfaces respectively, are of particular interest. Around this latitude the vertical distribution of salinity from station curves (not included in this paper) shows a salinity minimum below the surface of 200 cl/t with values ranging from 34·6°/$_{oo}$ at 110°E to less than 35·1°/$_{oo}$ at 53°E. In order to indicate the westward extent of low-salinity water on 160 cl/t surface, the isohaline of 35·1°/$_{oo}$ is drawn with dashes. The salinity in the low-salinity tongue increases westward from values less than 34·6°/$_{oo}$ at 110°E to values less than 35·1°/$_{oo}$ near the coast of Malagasy (figure 6a). This increase in salinity suggests that the low-salinity tongue is maintained by a west-ward transport of low-salinity water in the South Equatorial current, because the low-salinity water in the tongue is distinctly separated from the high-salinity waters of the north and south of the tongue. Furthermore, the salinity minimum in the western equatorial Pacific is conspicuous at about 160 cl/t (Tsuchiya 1968, figure 1a), with salinity less than 34·6°/$_{oo}$, and the low-salinity tongue must be the consequence of the Pacific Ocean water. The water in this tongue is characterized vertically by a salinity minimum. The vertical salinity minimum may be seen most clearly on the vertical sections along the various longitudes, in the International Indian Ocean Expedition Atlas (Wyrtki 1971, pp. 412, 440, 464, 497, 506, 510, 512). The low-salinity tongue, therefore, is not a result of vertical mixing but indicates that the low-salinity water from the Pacific is flowing westward with the South Equatorial Current. As the low-salinity water flows westward, replenishment of salinity by lateral mixing with the high-salinity water from the west takes place increasing the salinity to values exceeding 35·2°/$_{oo}$, in the west.

The sharp meridional gradient, south of the low-salinity tongue, is developed because the low-salinity water from the east is carried by the South Equatorial Current while the high-salinity water from the west is carried by the South Equatorial Countercurrent. The latitudinal belt, within which sharp meridional gradient is developed, coincides with the northern boundary of the South Equatorial Countercurrent (figures 6a, 7a).

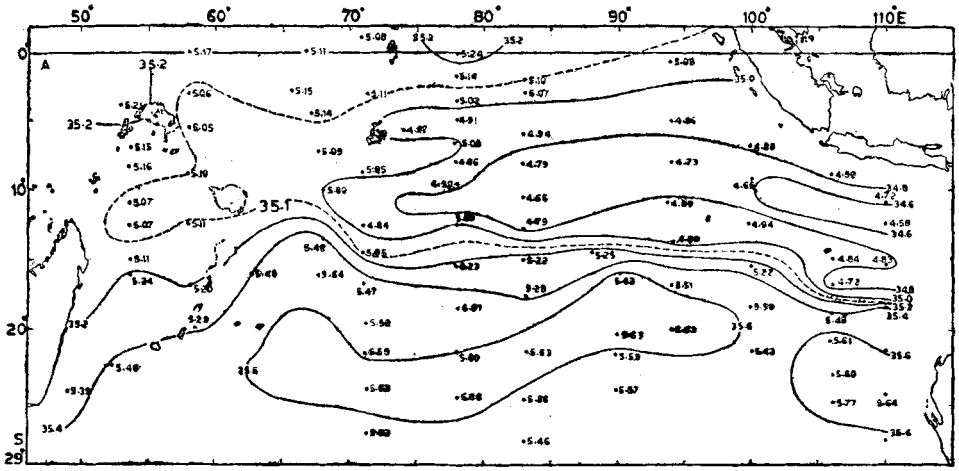

(a)

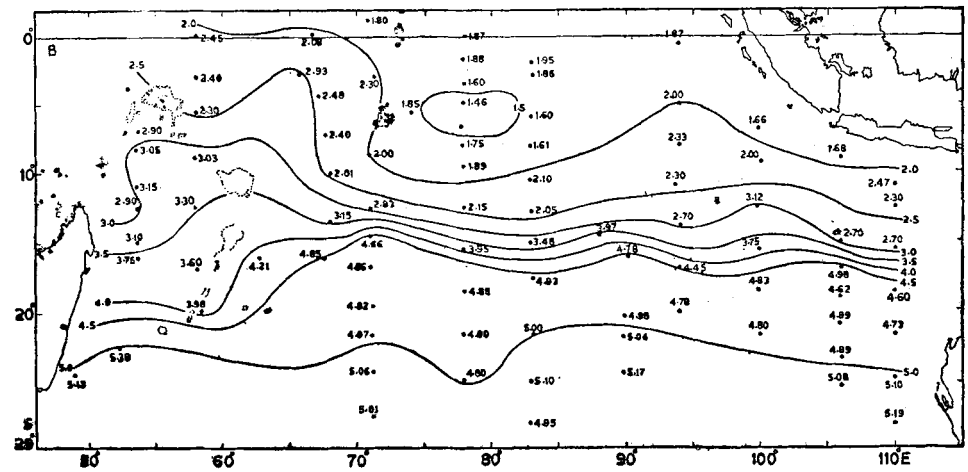

(b)

Figure 6. Salinity in per mille (a) oxyty in ml/l (b) at $\delta_\theta = 160$ cl/t.

The southward intrusion of low-salinity water marked by the 34·9°/$_{oo}$ isohaline near the coast of Malagasy on 120 cl/t surface suggests the southward branching of the South Equatorial Current flowing along the Malagasy coast.

Marked changes are noticed in the salinity distribution on 80 and 60 cl/t surfaces from that of 160 and 120 cl/t surfaces. The low-salinity tongue disappears on the surfaces of 80 cl/t and 60 cl/t. In contrast, high-salinity water from the northern hemisphere intrudes into the eastern Archipelago indicating the high-salinity water of the northern hemisphere, probably, enters the Pacific through the Banda and Timor seas at deeper depths to compensate the flow into the Indian Ocean. Consistent with this conclusion, relatively high-salinity water is noticed in the western equatorial Pacific on 80 cl/t surface (Reid 1965).

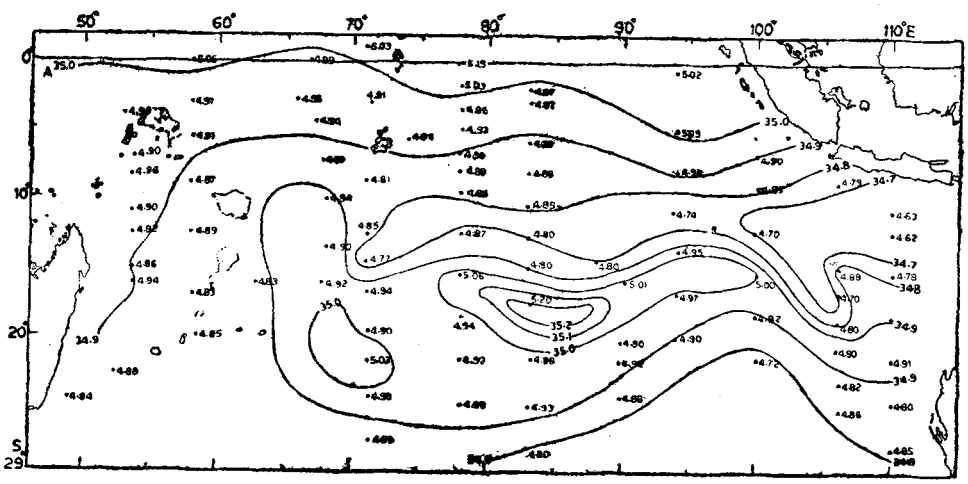

(a)

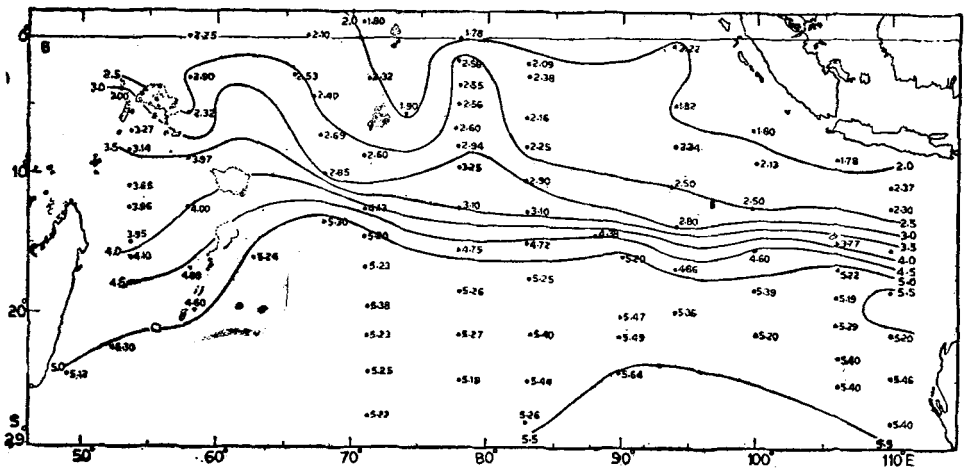

(b)

Figure 7. Salinity in per mille (a) oxyty in ml/l (b) at $\delta_\theta = 120$ cl/t.

3.4. *Oxyty*

Similar to the distribution of other properties, the distribution of oxyty on 80 and 60 cl/t is almost similar while that on 160 and 120 cl/t surfaces is similar. The major features of oxyty distribution as well as the distribution of other properties on 160 cl/t surface resemble those on 200 cl/t surface (Sharma 1972). The oxyty decreases continuously northward on all the surfaces. A sharp meridional gradient is developed on the surfaces of 160 cl/t and 200 cl/t in the east. In contrast to the upper two surfaces, the meridional gradient on 80 and 60 cl/t surfaces, particularly in the east, is very weak. The meridional gradients in oxyty and salinity distributions coinicde with the trough depicted by the depth contours on the surface of 160 cl/t where the South Equatorial Countercurrent in the central region is displayed on the acceleration

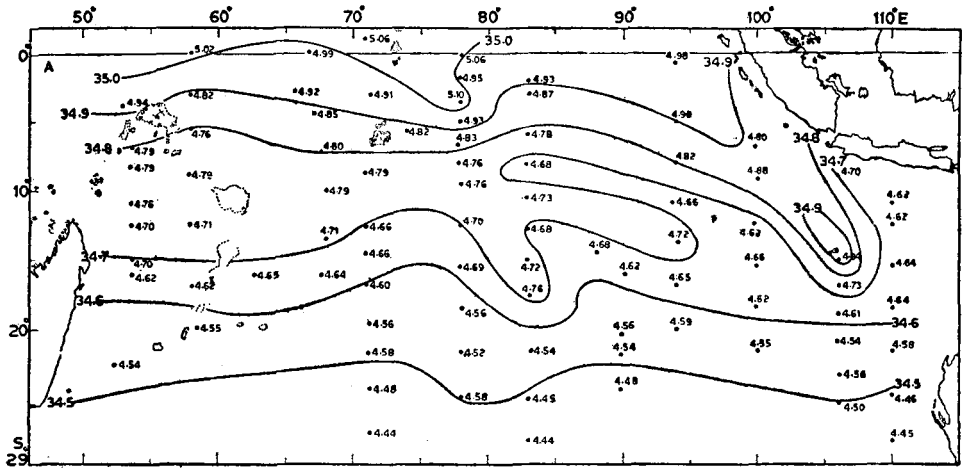

(a)

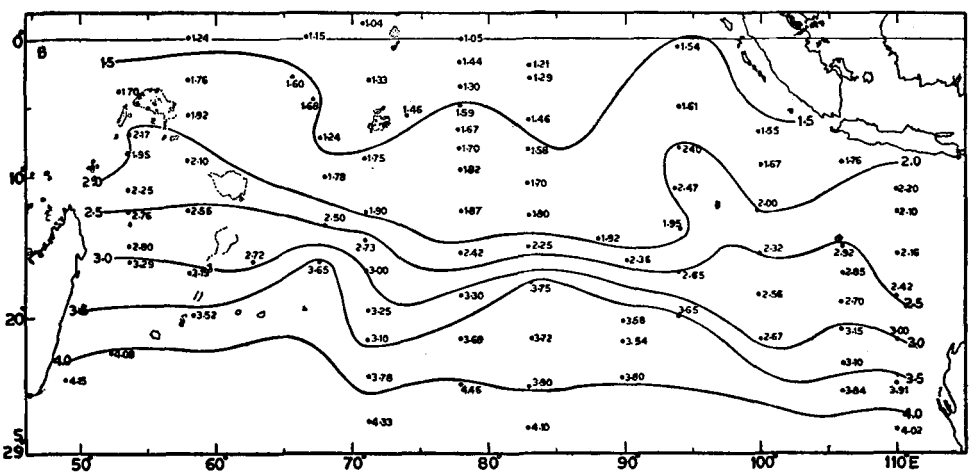

(b)

Figure 8. Salinity in per mille (a) oxyty in ml/l (b) at $\delta_\theta = 80$ cl/t.

potential chart. As the water from the east flows, due to lateral mixing with high-oxyty water of the south, there is an increase in oxyty in the west.

Far down stream of the South Equatorial Current, the oxyty values west of 70°E are higher in the north and lower in the south than at those latitudes in the east as indicated by the diverging oxypleths on 160 and 120 cl/t surfaces. Note that the area of spreading to the north is more than that to the south. This distribution suggests that the South Equatorial Current on these surfaces discharges more water to the north than to the south (figures 6b, 7b).

4. Zonal flow along 84°E

Eastward components, representing the Equatorial Countercurrent are found at the northern periphery of the section (figure 10). The magnitude of this current is

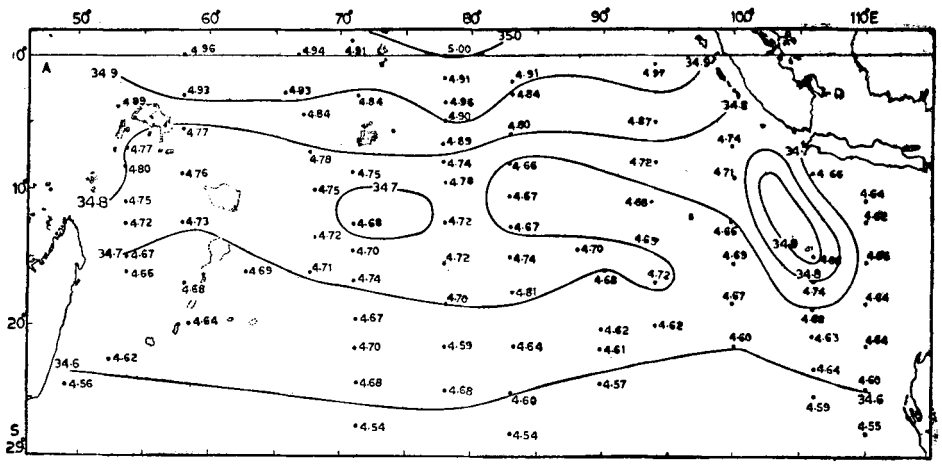

(a)

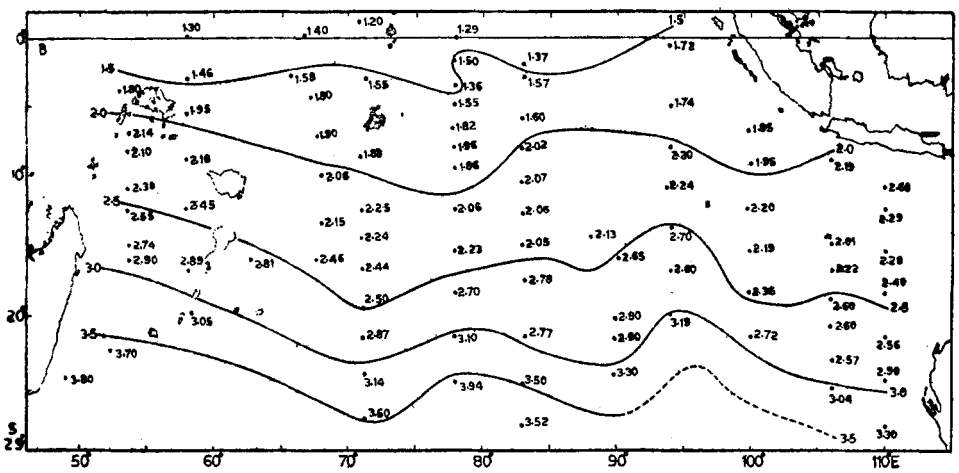

(b)

Figure 9. Salinity in per mille (a) oxyty in ml/l (b) at δ_θ=60 cl/t.

50 cm/sec in the surface layers. On this section, only a small cross section of the Equatorial Countercurrent to a depth of about 150 m, bounded by the South Equatorial Current at about 6° S is noticed. Between 8° S and 10° S, underneath the westward flowing South Equatorial Current, an easterly current lies. The ridge on the depth distribution at 160 and 120 cl/t surfaces is associated with the boundary of the easterly flow. The mean zonal component of the South Equatorial Current on this section is about 30 cm/sec and it agrees well with that of the zonal component at 65° E (Sharma 1976a).

The South Equatorial Countercurrent between 13°S and 15°S is conspicuous as a narrow band of an easterly flow within the broad South Equatorial Current system. The strength of this current on this section appears to be somewhat fortuitous, indicating a relatively high value in the surface, and it is probably because of an

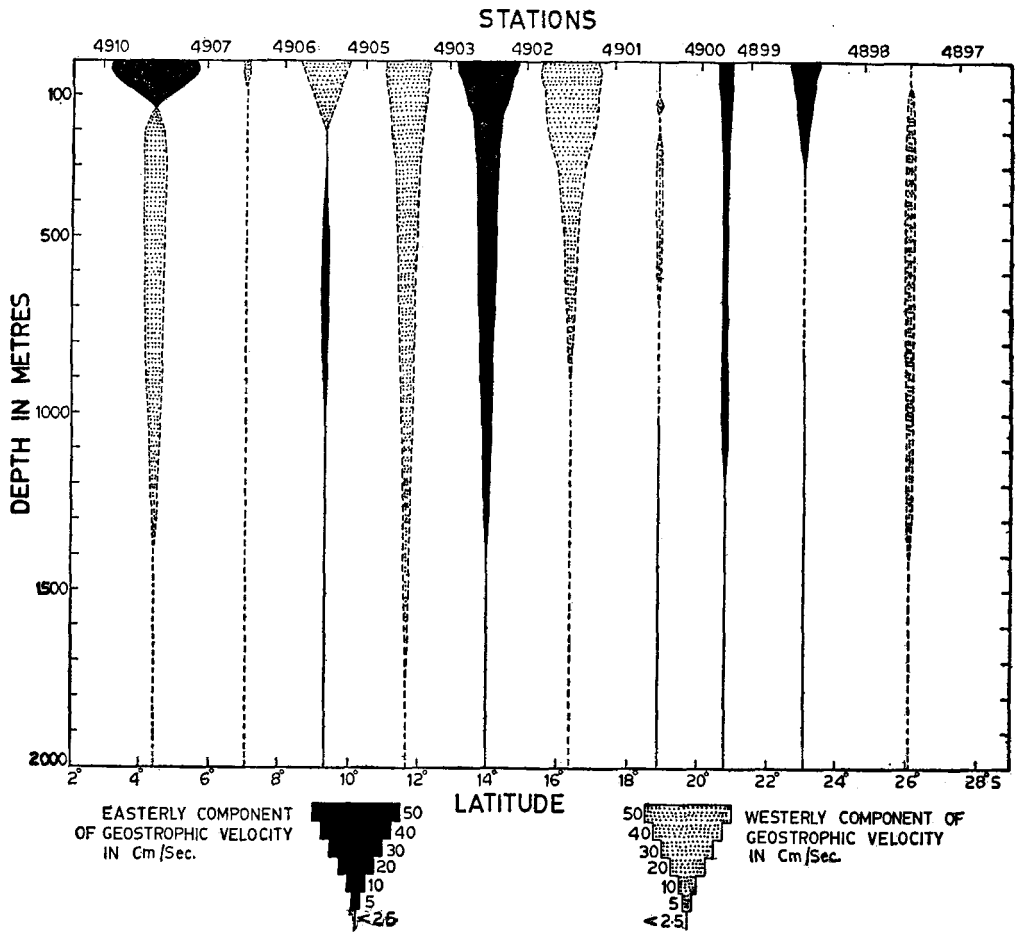

Figure 10. Zonal components of the geostrophic velocity at 84°C in cms/sec.

abnormally low value of dynamic height at *Vityaz* station 4902. Table 2 represents the zonal components of this current along two neighbouring meridional stations on either side at 78°E and 94°E. On Sharma's map at 65° E its strength at the surface is about 20 cm/sec and located at about 13°S (Sharma 1976a) whereas at 51°E it is located at about 10°S and its magnitude at the surface is 50 cm/sec (Premchand and Sastry 1976). The magnitude of this current at subsurface depths below 100 m at all the sections is almost of similar magnitude. The latitudinal position of the South Equatorial Countercurrent varies with longitude and shifts towards south as it flows eastward.

The Tropical Countercurrent which is again an easterly current is located between 20°S and 24°S. The width and magnitude of this current on the section at 84°S is almost similar to that at 65°E and it is slightly shifted northward at 84°E relative to that at 65°E (Sharma 1976a). A north-south inclination of this current with the latitudinal belt is evident from the acceleration potential charts at surfaces of 80 cl/t and 60 cl/t.

Table 2. Zonal components of the geostrophic currents (cm/sec.) relative to 2,000 db, along 78°E and 94°E (Positive-Eastward, Negative-Westward)

Depth in *m*	Along 78°E		Along 94°E	
	12°30′S-14°03′S	14°03′S-15°27′S	12°29′S-13°51′S	13°51′S-15°27′S
0	21·6	5·3	14·6	21·3
10	21·4	5·1	15·0	20·6
20	21·1	4·8	15·4	19·7
30	20·9	4·3	16·0	18·8
50	20·9	2·2	16·3	17·6
75	20·6	− 2·9	16·3	16·7
100	17·7	− 7·1	17·1	14·9
125	13·1	− 8·5	17·1	11·7
150	10·2	− 8·5	16·7	8·4
200	8·8	−10·2	14·4	5·3
250	7·8	− 3·2	13·1	3·9
300	6·8	0·0	12·9	2·7
400	4·8	3·9	11·2	1·4
500	3·2	5·6	9·9	1·7
600	2·4	6·6	10·5	1·7
700	1·7	7·7	10·3	1·4
800	1·0	7·7	9·9	0·6
900	0·3	7·1	9·7	− 0·2
1000	− 0·3	6·6	9·3	− 0·6
1100	− 0·9	5·6	9·5	− 1·5
1200	− 1·0	4·8	9·9	− 2·4
1300	− 1·2	3·9	9·7	− 2·9
1400	− 1·2	2·9	8·9	− 2·9
1500	− 1·0	2·0	7·6	− 2·6
1750	− 0·3	0·3	3·8	− 1·2
2000	0	0	0	0

5. Discussion

The isolines of depth, acceleration potential, salinity and oxyty in the southern region under study run almost parallel to the latitudes indicating the flow at these latitudes should be essentially zonal. Based on a similar distribution of depth, salinity and oxyty, Taft (1963) concluded that there is no clear evidence of northward transport of low-salinity waters. Sharma (1976b) discussed in detail the trans-equatorial movement of water masses in the Indian Ocean and concluded that the transequatorial exchange of water masses is limited to very near the coasts.

Based on salinity minimum on the meridional profiles Tchernia *et al* (1958) inferred that the Antarctic Intermediate Water enters the North Indian Ocean crossing the equator and the low-salinity water in the Northwest Indian Ocean is attributed to the Antarctic Intermediate Water. But Taft (1963) pointed out that the salinity minimum in the region north of equator and the Antarctic Intermediate Water are not in a line of flow because they are at different steric levels, and concluded that the Antarctic Intermediate Water cannot be the source of the salinity minimum. Warren *et al* (1966) remarked that this condition cannot preclude a southern origin for the fresh water at depths less than those of the core of the Antarctic Intermediate Water and suggested that the shallow, northward moving Subtropical Subsurface Water lies above the high-salinity core of the North Indian Ocean Water and penetrates north of equator. As proposed by Warren *et al* (1966), if the low salinity Subtropical Subsurface Water were to penetrate north of equator, a salinity minimum in the vertical distribution of salinity should have been present all along the equator at levels where

this water crosses the equator. A cursory glance of station curves along the equator reveals the absence of salinity minimum, and on the other hand vertical spreading of homogeneous water in the depth range of 100 to 1,000 m is conspicuous (Sharma 1972, 1976a). Furthermore, a close examination of meridional sections indicates the absence of any transequatorial flow except very near the coasts (Wyrtki 1971; Sharma 1976a) and this inference has been further confirmed by Sharma (1976b). As mentioned earlier, the orientation of isolines in the southern region shows zonal flow and hence, the possibility of any meridional flow in the southern Indian Ocean can be ruled out. As such, the South Indian Ocean cannot be the source of low-salinity water in the northwestern Indian Ocean. On the other hand, the distribution of salinity on the surface of 160 cl/t and 120 cl/t (figures 6a, 7a) clearly demonstrates the low-salinity tongue emanating from the Eastern Archipelago. The characteristics of the water in the tongue are similar to those of the Equatorial Pacific Ocean Water (Tsuchiya 1968). The salinity distribution on other steric levels above 100 cl/t is in conformity with this feature (Rochford 1958; Taft 1963; Wyrtki 1971; Sharma 1972). Hence, the water appears to come southward from the Pacific Equatorial Currents by way of Banda and Timor seas, and penetrates the more saline water of the Indian Ocean as far west as 53 E° (figure 6a). West of 53°E, spreading of this water is obvious from the distribution of properties on 160 and 120 cl/t surfaces.

Taft (1963) attributed the low-salinity water in the northwestern Indian Ocean to the Pacific Ocean origin. Warren *et al* (1966) questioned this inference on the ground that the oxyty of the water coming from the Banda Sea is 2·3 ml/l and not over 2·5 ml/l while that of the low-salinity water in the northwestern Indian Ocean is more than 3·0 ml/l. Sharma (1972) contradicted this argument based on the fact that the difference in oxyty of the waters in the Somali Basin and the Eastern Archipelago is much less (less than 0·5 ml/l) and it is probable that the oxyty of the water is increased through mixing with the high-oxyty water from the south during its flow to the west.

In a recent paper Premchand and Sastry (1976) while discussing the origin of the low-salinity water in the western Indian Ocean agreed with the absence of a direct line of flow of the South Indian Ocean Water (Antarctic Intermediate Water or the Subtropical Subsurface Water). However, they disagree with the point of view that this water is from the Pacific Ocean. They also disagree with the argument of Sharma (1972) that the higher oxyty in the Somali Basin over the Pacific Ocean Water is due to mixing with the higher-oxyty water of the south during its flow. They remarked ' If oxyties were to increase from 2·3 ml/l in the eastern Indian Ocean to 3·3 ml/l in the Somali Basin by mixing of high-oxyty waters (say, of oxyty 4 ml/l) with the waters of Pacific origin in equal volumes, the mixture still possesses lower oxyties than those observed in the Somali Basin.' The oxyty values over 3·3 ml/l which these authors reported are the maxima of oxyty not in the salinity minimum but 100 to 150 m above salinity minimum in the Somali Basin which is evident from Warren *et al* (1966 p. 840) who stated Near the continental slope on Profiles A and B (figures 3 and 4) the oxygen maximum exceeds 3·0 ml/l but lies some 150 m above the salinity minimum. Elsewhere, except at Sta. 45 (figure 5) and at Sta. 67 (figure 8) are comparably high values seen, and except at Sta. 67, the vertical separation between the oxygen maximum and the salinity minimum is smaller than on Profiles A and B, less than 100 m. The high oxygen layer is least apparent on Profile F (figure 8); at Stas. 64 and 65, where there is a well-developed salinity minimum, there is only a faintest indication of an oxygen maximum in the serial observations (none in the isopleths)'. Furthermore,

the value of oxyty in the Equatorial Pacific Ocean Water which penetrates into the Indian Ocean south of 10°S through the Banda and Timor seas on and above 100 cl/t. surface is not less than 2·5 ml/l (Taft 1963; Reid 1965; Tsuchiya 1968). Hence, the increase in oxyty of the Pacific Ocean Water is not more than 0·5 ml/l through mixing with the higher-oxyty water of the south. Further, the process of mixing is accelerated by the shear developed due to the presence of the South Equatorial Countercurrent at about 13°S which flows in the opposite direction to that of the South Equatorial Current along which the Pacific Ocean Water is carried (Sharma 1976a). On the contrary, as suggested by Premchand and Sastry (1976) if the Antarctic Intermediate Water which shows the oxyty to be 5·5 ml/l at 100 cl/t at the two *Vityaz* stations 5182 and 5184 just above the salinity minimum were to be drawn into the Somali Basin along the West Australian Current, and if we assume the mixing takes place with the water having the lowest value of 2·5 ml/l oxyty and equal proportion of these two waters, the resulting mixture should not have the oxyty less than 4·0 ml/l. Another point of view expressed by these authors to show that the low-salinity water is not from the Pacific Ocean is the absence of salinity minima at *Diamantina* station (2/62) 86 at 7° 41′ S; 105° 01′ E and *Vityaz* station (35) 5184 at 21° 45·2′ S; 108° 26·3′ E. Primarily, it should be noted that the Pacific Ocean Water enters the Indian Ocean only south of 10° S through Banda and Timor seas. Hence the water characteristics at Dm (2/62) 86 cannot be representative of the Pacific Ocean Water. Secondly, the salinity minimum can be conspicuous if the low-salinity water is sandwiched between two high-salinity waters. The Pacific Ocean Water in the eastern Indian Ocean is characterized only as a vertical extent of low-salinity water above 100 cl/t. As this water mass moves westward, in the Somali Basin it is sandwiched between the two salinity maxima arising out of the Red Sea and Persian Gulf waters which are present on the isanosteres below 100 cl/t and above 120 cl/t respectively. As suggested by Premchand and Sastry (1976) if the Antarctic Intermediate Water is to be carried along with the West Australian Current, the isohalines as well as the isolines of acceleration potential should have shown a meridional orientation instead of zonal orientation which, obviously, indicates the absence of the Antarctic Intermediate Water above 100 cl/t surface north of the South Equatorial Countercurrent.

The salinity structure on the meridional sections (Wyrtki 1971) indicates a break up between 15° S and 10° S, with low-salinity water separating the high-salinity waters from the north and south. The characteristics of this water in the break up are similar to those of the Equatorial Pacific Ocean Water (Tsuchiya 1968).

On 80 and 60 cl/t surfaces incursion of the Pacific Ocean Water is not noticed and on the converse, the North Indian Ocean Water penetrates towards the Eastern Archipelago as a high-salinity tongue (figures 8a, 9a).

A first glance of the distribution of acceleration potential as well as the depth and salinity maps gives an impression that the distribution in these properties is markedly changed in the Archipelago region because of a few stray values at the Umitaka Maru stations. But a closer examination of the T-S curves shows that the varation is consistent with the observations at neighbouring stations covered by other vessels.

6. Conclusion

Low-salinity water from the Pacific Ocean intrudes into the western Indian Ocean

along the South Equatorial Current, in the layers above 100 cl/t. Below 100 cl/t relatively higher-salinity water of the North Indian Ocean appears to penetrate into the Eastern Archipelago and ultimately into the Pacific Ocean. However, further studies are to be carried out with more data in the Eastern Archipelago region to confirm the incursion of the North Indian Ocean Water into the Pacific Ocean.

The low-salinity water in the northwestern Indian Ocean at intermediate depths has its origin in the Pacific Ocean. Neither the Antarctic Intermediate Water nor the Subtropical Subsurface Water enter the North Indian Ocean except very near the coasts.

The South Equatorial Countercurrent and the Tropical Countercurrent are found at 12° S–15° S and 20° S–24° S respectively. The latitudinal position of these currents vary with longitudes.

Acknowledgements

The authors wish to thank Joseph L. Reid, Scripps Institution of Oceanography, La Jolla, California, for going through the manuscruipt and making valuable suggestions for improvement.

References

Helland-Hansen B 1930 *Rep. Sars. N. Atl. Deep-Sea Exped.* **1** 317
Montgomery R B 1937 *Bull. Amer. Met. Soc.* **8** 276
Montgomery R B and Spilhaus A F 1941 *J. Aero. Sci.* **18** 210
Montgomery R B and Stroup E D 1962 *Johns Hopk. Oceanogr. Stud.* **1** p. 68
Premchand K and Sastry J S 1976 *Indian J. Mar. Sci.* **5** 169
Reid J L 1959 *Nature (London)* **184** 209
Reid J L 1965 *Johns. Hopk. Oceanogr. Stud.* **2** p. 85
Rochford D J 1958 *J. Mar. Res.* **17** 483
Sharma G S 1972 *J. Mar. Res.* **30** 102
Sharma G S 1976a *J. Oceanogr. Soc. Jpn.* **32** 284
Sharma G S 1976b *J. Mar Res.* **43** 143
Sverdrup H U, Johnson M W and Fleming R H 1942 *The oceans: their physics, chemistry and general biology* (New York: Prentice-Hall) p. 1087
Taft B A 1963 *J. Mar. Res.* **21** 129
Tchernia Paul, Lacombe H and Guibout P 1958 *C.O.E.C. Bull. d' Inform.* **10** 115
Tsuchiya M 1968 *Johns Hopk. Oceanogr. Stud.* **4** p. 50
Uda M and Hasunuma K 1969 *J. Oceanogr. Soc. Jpn.* **25** 201
Uda M and Nakamura Y 1973 *Spl publ. Mar. Biol. Ass. India* 276
Warren B, Stommel H and Swallow J C 1966 *Deep-Sea Res.* **13** 825
Wyritki Klauss 1957 *Proc. 9th Pacif. Sci. Congr.* **16** 61
Wyrtki Klauss 1971 *Oceanographic Atlas of the International Indian Ocean Expedition National Science Foundation*, Washington p. 531.
Yoshida K and Kidokoro T 1967a *J. Oceanogr. Soc. Jpn.* **23** 88
Yoshida K and Kidokoro T 1967b *J. Oceanogr. Soc. Jpn.* **23** 231